ELSEVIER

Magnetic Resonance Imaging 20 (2002) 521–525

MAGNETIC RESONANCE IMAGING

BOLD signal compartmentalization based on the apparent diffusion coefficient

Allen W. Song[a,b]*, Harlan Fichtenholtz[b], Marty Woldorff[b]

[a]*Brain Imaging and Analysis Center*
[b]*Center for Cognitive Neuroscience, Duke University, Durham, NC 27710, USA*

Received 4 February 2002; accepted 27 May 2002

Abstract

Functional MRI (fMRI) can detect blood oxygenation level dependent (BOLD) hemodynamic responses secondary to neuronal activity. The most commonly used method for detecting fMRI signals is the gradient-echo echo-planar imaging (EPI) technique because of its sensitivity and speed. However, it is generally believed that a significant portion of these signals arises from large veins, with additional contribution from the capillaries and parenchyma. Early experiments using diffusion-weighted gradient-echo EPI have suggested that intra-voxel incoherent motion (IVIM) weighting inherent in the sequence can selectively attenuate contributions from different vessels based on the differences in the mobility of the blood within them. In the present study, we used similar approach to characterize the apparent diffusion coefficient (ADC) distribution within the activated areas of BOLD contrast. It is shown that the voxel values of the ADCs obtained from this technique can infer various vascular contributions to the BOLD signal.

Keywords: fMRI; BOLD; Diffusion weighting; ADC

1. Introduction

The development of functional MRI [1–6] (fMRI) has given neuroscientists a new powerful tool to non-invasively detect neuronal activation. Because the observed hemodynamic responses are secondary to neuronal activity, they are generally believed to provide a good spatial measure of the location of the activated brain areas. However, the detected fMRI signals were based on the blood oxygenation level dependent (BOLD) contrast [7], thus they could arise from vasculature of all sizes; some of them could be distant from the neuronal activity. Therefore, understanding the origins of these signals is important in determining the true spatial relationship between the observed fMRI signals and the neuronal activities. In the past decade, although functional MRI (fMRI) has seen extensive development in its application in neuroscience, the spatial accuracy of the BOLD signal localization remains questionable because of confounding signals from relatively distant vasculature.

The present study was designed to assess the functional signal components according to their apparent mobility within the activated areas using the traditional BOLD contrast. Such an assessment is made possible by using an interleaved diffusion weighting method with various *b* factors to allow derivation of the ADCs while assessing BOLD activation. Isotropic diffusion weighting was used to achieve a consistent measure of the apparent diffusion coefficients independent of the patient orientation. To gain better sensitivity, the study was carried out on a 4T MRI scanner.

2. Methods

It is well known that diffusion weighting can be used to selectively attenuate MR signals from proton pools undergoing diffusion process. The signal attenuation is governed by the equation

$$S = So * e^{-bD} \quad (1)$$

where *So* is the original signal, *S* the signal after attenuation, *D* the apparent diffusion coefficient (ADC) and *b* the diffusion weighting factor. The ADC indicates the mobility of the proton pools. The *b* factors of the diffusion weighting

* Corresponding author. Tel.: +1-919-684-1215; fax: +1-919-681-7033.
E-mail address: allen.song@duke.edu (A.W. Song).

0730-725X/02/$ – see front matter
PII: S0730-725X(02)00516-7

are dependent on the duration of the weighting time and the amplitude of the weighting gradients. In principle, they are proportional to the cube of the time and the square of the gradient amplitude. Equation [1] indicates that more signal attenuation will be resulted from larger D and b factors. By fitting the images without and with diffusion weighting, ADCs can be obtained which may reflect the mobility.

To ensure spatially homogeneous attenuation of the signal from the brain tissue that is independent of the subject orientation, an isotropic diffusion weighting method was used [9]. The isotropic diffusion weighting gradients were embedded into a gradient-recalled spiral imaging sequence [11,12]. The use of spiral acquisition allowed us to achieve large b factors without using excessively long echo time in that spiral imaging starts data acquisition from the center of k-space. The final pulse sequence was implemented on a General Electric 4T whole-body MRI scanner (Milwaukee, Wisconsin) running on the LX platform.

Functional signal was generated using a simple motor paradigm of finger opposition. Subjects were instructed through the scanner audio interface to bilaterally and sequentially tap their fingers, starting with a resting state, for three and a half on/off cycles while the time-course volumes were acquired continuously (at a rate of one volume per second). Each volume contained five axial slices of a 64×64 matrix at FOV of 24 cm through the motor cortex. A total of 210 volumes were acquired in each run of three minutes and thirty seconds duration at the TR of 1 s and TE of 50 ms.

In order to dynamically visualize the contributions from different vessels, a ramped diffusion-weighting scheme was adopted. That is, the b factors of the diffusion weighting were cyclically varied from one acquisition to the next so that the MR signals were attenuated in a cyclic fashion. The b factors for diffusion weighting were varied cyclically between three values in the three-second cycle: 0, 114 and 229 s/mm^2. A total of seventy such cycles was acquired for each run. Four runs were acquired for each subject, which were then averaged together to gain statistical power. Because a dynamic run was acquired that contains many such cycles, the attenuation would result in cyclic fluctuations of the signal. Consequently, MR signal from proton pools of high mobility (e.g., large vessels) would be manifested as large fluctuations in the signal time course at the imposed diffusion-weighting cycling frequency, which was one cycle per every 3 acquisitions. Since the acquisition rate/TR was one acquisition per second, the temporal frequency of this cycling was one cycle per every three seconds.

The dynamic time-course images of the cycling diffusion weighting can be sorted based on the b factors. That is, for each given b factor, a separate time course can be used to assess the effect of that diffusion weighting on the functional signal. Note, then, that for the samples with a b factor of zero, the time course is entirely based on the BOLD contrast. Activated areas based on the BOLD time courses were found via a multiple regression algorithm, which can also effectively remove the linear drift commonly seen in the time course. Within the activated areas indicated by the BOLD contrast (i.e., using the BOLD activation as a mask), the mean ADC value for each pixel across all the runs was also calculated. This information allows the categorization of the BOLD signal origin based on different mobility, which can be used, in turn, to infer various vascular origins. Within the BOLD activated areas, ADCs were obtained for each pixel. These pixels were then pseudo-colored based on their ADC values.

All images were acquired in the form of raw data (i.e., data before Fourier transformation), which were transported to an SGI Octane workstation (Mountain View, California) for off-line reconstruction. A regridding algorithm in the k-space was used to interpolate the data to Cartesian space, and a standard fast Fourier Transform was then performed to arrive at the final images. All images were concatenated into volume format, and time courses were analyzed on a pixel-by-pixel basis.

3. Results and discussion

Six subjects were recruited under written consent approved by the Institute Review Board of the Duke University. All experiments were carried out at 4T whole-body MRI scanner (GEMS, Milwaukee, Wisconsin).

A typical data set with the ramped diffusion weighting is presented in Fig. 1. The images are shown in (a) and the time courses from a given region of 25 voxels (indicated as a red square in (a)) in primary motor cortex are shown in (b). Because of the cyclically varied diffusion weighting during each run, the mobility of the proton pools is clearly manifested as rapid cyclic fluctuations of the time course (one period every three seconds). The more mobile a particular proton pool is, the larger this fluctuation would be in the time course, which can be clearly seen in the representative 25-pixel array taken from the motor cortex. In principle, protons pools can be approximately divided into the following groups: [1] non-activated large vessels (e.g., pixel 16), with large fluctuations at the high (i.e., diffusion-cycling) frequency (one cycle per every 3 sec), but with no variation at the lower (i.e., task-cycling) frequency (one cycle every 60 sec), [2] non-activated small vessels (e.g., pixel 13), with small high-frequency diffusion related fluctuations and no task-frequency variation, [3] non-activated parenchyma (e.g., pixel 10), with very small high-frequency fluctuations and no task-frequency variation, [4] activated large vessels (e.g., pixel 23), with large high-frequency fluctuations AND large task-frequency variation, [5] activated small vessels (e.g., pixel 24), with small high-frequency fluctuations but large task-frequency variation, and [6] activated parenchyma (e.g., pixel 25), with very small high-frequency fluctuations but large task-frequency variation. It is evident that partial volume effects will complicate the interpretation of activity in small vessels—that is, a

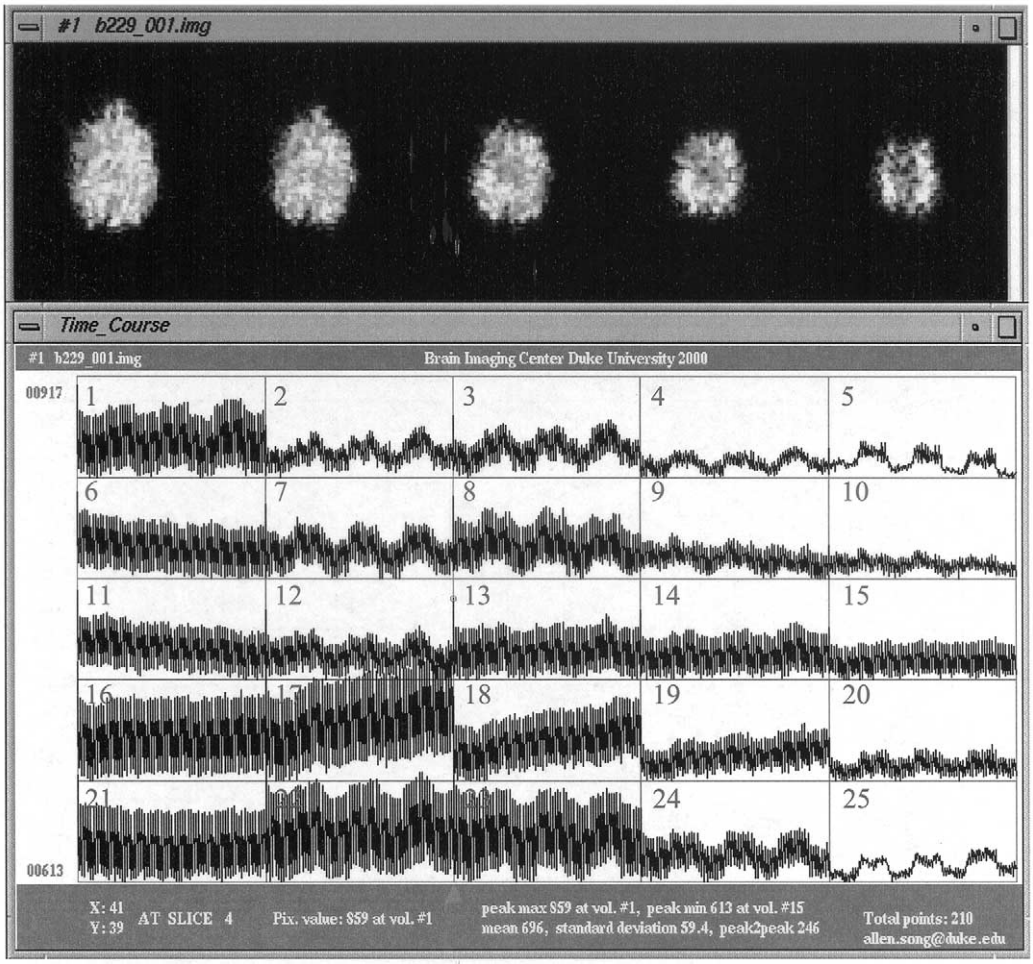

Fig. 1. Spiral images using isotropic diffusion weighting in the presence of cyclically varying *b* factors. The times courses over 210 seconds were taken from a 25-pixel array indicated in the red square in the image. The high-frequency signal oscillation (at 0.33 Hz) is caused by the cyclically varying diffusion weighting, whereas the much lower frequency variation (low frequency envelope) is caused by the task alternation between finger-tapping and rest every 30 sec. The different amplitudes seen for signal variations at these two frequencies reflect the different contributing proton pools for each pixel.

mixture of large vessel and parenchyma proton pools may lead to an appearance that resembles the small vessels. Further investigation using higher spatial resolution would reduce this partial volume effect and help to achieve finger categorization. However, if these clusters of pixels surround an identified large vessel (areas colored in blue), it is likely that these areas are contaminated by partial volume effect. Activated pixels that have no large vessel in the vicinity would more likely arise from capillary origins.

A multiple regression algorithm was run on the samples in the EPI time course that had no diffusion weighting (i.e., the $b = 0$ samples). Regressors containing the activation paradigm and linear function were used to obtain the BOLD activation maps while effectively removing the linear drifts. Fig. 2(a) shows the activated pixels based on the BOLD contrast from these data. Within the activated areas based on the BOLD contrast, the mean ADCs were calculated. Three pools were inferred in this report, based on previously reported apparent diffusion coefficients [10,13–15]. The activated pixels with apparent diffusion coefficients of less than 0.8×10^{-3} mm^2/s were considered to be of parenchyma origin, the pixels with diffusion coefficients of more than 2.2×10^{-3} mm^2/s were considered to be from large vessels, while everything in between was treated as small vessels, CSF, or a mixture of large vessels and parenchyma. The cut-off value for the lower limit for this categorization was based on the diffusion coefficients of the parenchyma, which is in general smaller than 0.8×10^{-3} mm^2/s. The upper limit is based on the diffusion coefficient of CSF (similar to free water), which is approximately 2.2×10^{-3} mm^2/s, and thus pools with diffusion coefficient larger than 2.2×10^{-3} mm^2/s were treated as large vessels. On average across all subjects, under such a categorization scheme, it was calculated that 18.6% of the total activated pixels were from large veins, 62.4% from small vessels (including capillaries) and CSF (because of its medium ADC value), and 19% from parenchyma. Note that the compartment that is labeled small vessels and CSF could also contain mixture of the parenchyma signal. Fig. 2(b) shows a representative example of such characterization with activated pixels in

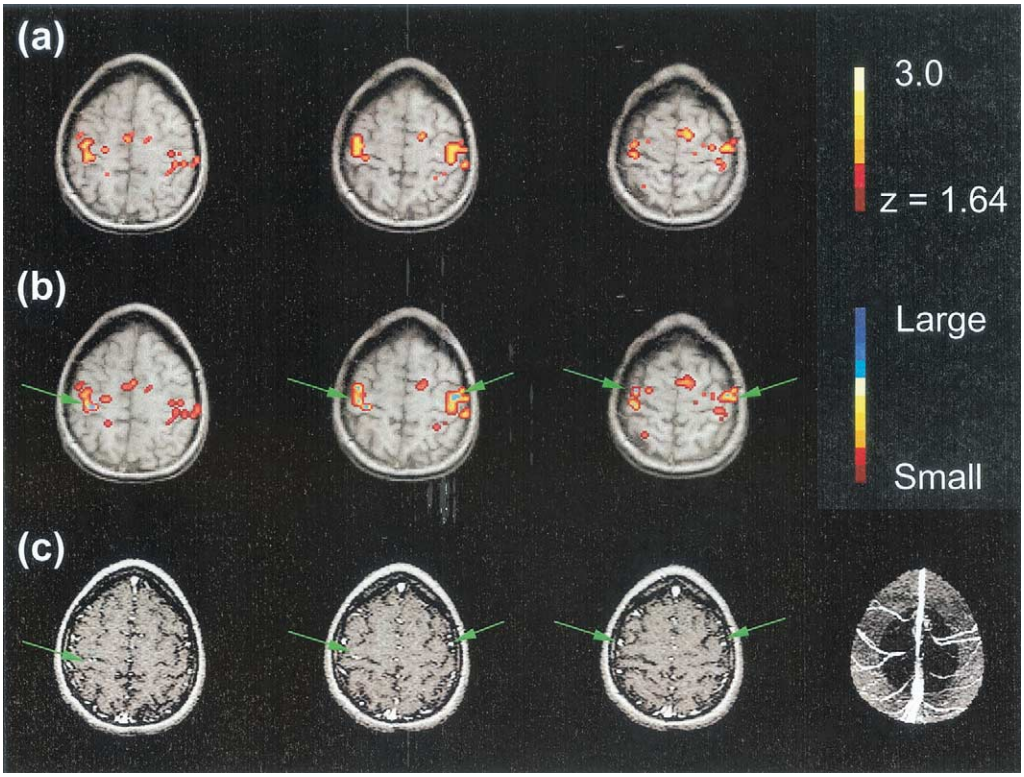

Fig. 2. (a) Activated area of BOLD contrast determined by statistical tests with linear detrending; the Z-score threshold was 1.64. (b) Categorization of signal origins within the activated areas based on the apparent diffusion coefficients, blue: large vessels (diffusion coefficient $> 2.2 \times 10^{-3}$ mm^2/s), orange: small vessels and CSF (diffusion coefficient in between 0.8 and 2.2 $\times$ 10^{-3} mm^2/s), red: parenchyma (diffusion coefficient $< 0.8 \times 10^{-3}$ mm^2/s), (c) MR time-of-flight angiogram taken from the same location, showing the location of the major vessels near or in the activated areas in motor cortex (green arrows). Note the spatial correspondence of these vessels to the proton-pool components indicated in (a) and (b).

color, with likely large-vessel contribution shown in blue, that from parenchyma in red, and that from small vessels in yellow. A more detailed breakdown of the specific components may require better spatial resolution and finer steps of diffusion weighting b factors.

To validate the categorization of the large vessels using the diffusion weighting method, an MR angiogram was taken at the same location shown in Fig. 2(c). Since the pial arteries and veins usually run next to each other, the location of large arteries corresponds well with that of large veins. The good spatial agreement between the large vessels in MR angiogram and the blue clusters in Fig. 2(b) indicates that the diffusion weighting method could be useful in categorizing BOLD signal with vascular origins.

This initial report demonstrates the possibility of providing good knowledge of the vascular origins of the functional signal and quantitation of the relative contribution from the various proton pools. For example, the activated areas immediately surrounding a blue cluster are likely due to the extra-vascular BOLD effect of a large vein in the surrounding parenchyma. This observation is not possible by the conventional use of the diffusion weighting methods that simply crush only the intra-vascular signal from the large veins. It is also seen that pixels from the large vessels do not necessarily show large BOLD signal, evidenced by the spatial decoupling between the pixels of high BOLD signal and pixels of high diffusion coefficients. Excluding the contributions from the large vessels and their surrounding areas, it is evident that the capillary and parenchyma contributions are significant at 4T.

4. Conclusions

We have demonstrated that the diffusion weighting methods can be used to characterize the ADCs within the activated areas based on the BOLD contrast. Such categorization of the various proton pools based on the mobility allows direct inference of various vascular origins to the BOLD signal, which would help identify and remove the confounding signals such as those from the large veins and their surrounding areas, and focus on the small vessel BOLD activation to improve spatial specificity.

Acknowledgments

The authors would like to thank Dr. Gary Glover at the Stanford University for the spiral imaging pulse sequence program on which the diffusion-weighting imaging sequence was built. The authors also wish to thank the finan-

cial support from the National Science Foundation (BES 0092672) and National Institutes of Health (MH 60415).

References

[1] Belliveau JW, Kennedy DN, McKinstry RC, Buchbinder BR, Weisskoff RM, Cohen MS, Vevea JM, Brady TJ, Rosen BR. Functional mapping of the human visual cortex by magnetic resonance imaging. Science 1991;254:716–9.

[2] Kwong KK, Belliveau JW, Chesler DA, Goldberg IE, Weisskoff RM, Poncelet BP, Kennedy DN, Hoppel BE, Cohen MS, Turner R, Cheng HM, Brady TJ, Rosen BR. Dynamic magnetic resonance imaging of human brain activity during primary sensory stimulation. Proc Natl Acad Sci USA 1992;89:5675–9.

[3] Bandettini PA, Wong EC, Hinks RS, Tikofsky RS, Hyde JS. Time course EPI of human brain function during task activation. Magn Reson Med 1992;25:390–7.

[4] Ogawa S, Tank DW, Menon R, Ellerman JM, Kim SG, Merkle H, Ugurbil K. Intrinsic signal change accompanying sensory stimulation: functional brain mapping with magnetic resonance imaging. Proc Natl Acad Sci USA 1992;89:5951–5.

[5] Menon R, Ogawa S, Tank DW, Ugurbil K. 4 Tesla gradient recalled echo characteristics of photic stimulation-induced signal changes in the human primary visual cortex. Magn Reson Med 1993;30:380–6.

[6] Turner R, Jezzard P, Wen H, Kwong KK, LeBihan D, Zeffiro T, Balaban RS. Functional mapping of the human visual cortex at 4 and 1.5 Tesla using deoxygenated contrast EPI. Magn Reson Med 1993; 29:277–9.

[7] Ogawa S, Menon RS, Tank DW, Kim SG, Merkle H, Ellerman JM, Ugurbil K. Functional brain mapping by blood oxygenation level dependent contrast magnetic resonance imaging. Biophys J 1993;64: 803–12.

[8] LeBihan D, Breton E, Lallemand D, Grenier P, Cabanis E, Laval-Jeantet M. MR imaging of intravoxel incoherent motions: application to diffusion and perfusion in neurologic disorders. Radiology 1986; 161:401–7.

[9] Wong EC, Cox RW, Song AW. Optimized isotropic diffusion weighting. Magn Reson Med 1995;34:139–43.

[10] Song AW, Wong EC, Tan SG, Hyde JS. Diffusion weighted FMRI at 1.5 T, Diffusion weighted FMRI at 1.5 T. Magn Reson Med 1996; 35:155–8.

[11] Ahn CB, Jim JH, Cho ZH. High speed spiral-scan echo planar NMR imaging. IEEE Trans Med Imag 1986;MI-5:2–7.

[12] Meyer CH, Mocovski A. Square spiral fast chemical shift imaging. Magn Reson Imag 1987;5:519.

[13] Conturo TE, McKinstry RC, Aronovitz JA, Neil JJ. Diffusion MRI: precision, accuracy and flow effects. NMR Biomed 1995;8(7–8): 307–32.

[14] LeBihan D, Turner R. The capillary network: a link between IVIM and classical perfusion. Magn Reson Med 1992;27:171–8.

[15] Zhong J, Kennan RP, Fulbright RK, Gore JC. Quantification of intravascular and extravascular contributions to BOLD effects induced by alteration in oxygenation or intravascular contrast agents. Magn Reson Med 1998;40(4):526–36.